Mon. Not. R. Astron. Soc. **344,** 1257–1263 (2003)

The young cluster in the CB34 globule: the clumps and the outflows

C. Codella[1]★ and F. Scappini[2]

[1]*Istituto di Radioastronomia, CNR, Sezione di Firenze, Largo E. Fermi 5, 50125 Firenze, Italy*
[2]*Istituto per lo Studio dei Materiali Nanostrutturati, CNR, Sezione di Bologna, Via P. Gobetti 101, 40129 Bologna, Italy*

Accepted 2003 June 11. Received 2003 June 9; in original form 2003 March 19

ABSTRACT

The molecular environment of the young cluster of Class 0 young stellar objects (YSOs) located in the globule CB34 has been investigated through a multiline millimetre survey. The CO, ^{13}CO, C^{18}O and CS emissions show that the present star-forming process is concentrated into three molecular clumps with the size of ∼0.25 pc, which are embedded in a cool more extended gas. The spatial distribution of the high-velocity emission reveals the occurrence of multiple outflows which are associated with the brightest YSOs.

The interaction of the outflows with the molecular clumps has been studied by using the abundances of products of shocked chemistry such as SiO and SO. The abundances of these molecules at the high velocities of the outflows can be used to further specify, with respect to the continuum results, the characteristics of the Class 0 YSOs. In particular, one of the YSOs which does not show the presence of SiO and SO at high velocities is thought to be in a more evolved phase where most of the molecules produced at high velocities in the shocked regions have been already destroyed.

Key words: ISM: clouds – ISM: globules – ISM: individual: CB34 – ISM: jets and outflows – ISM: molecules – radio lines: ISM.

1 INTRODUCTION

One of the best sites to study the star-forming process is represented by the Bok globules (Bok & Reilly 1947), which are relatively isolated and simple dark clouds generally hosting star formation (e.g. Clemens & Barvainis 1988; Clemens, Yun & Heyer 1991, and references therein). In particular, CB34 stands unique for its distance (1500 pc, according to Launhardt & Henning (1997), whereas the average value for Bok globules is ∼600 pc) and for its clear association with multiple star formation. Near-infrared (NIR) studies revealed reddened objects as well as a number of Herbig–Haro objects and H_2 jets (Alves & Yun 1995; Moreira & Yun 1995; Khanzadyan et al. 2002). The youngest star population has been recently mapped at 450 and 850 μm by Huard, Weintraub & Sandell (2000), who have discovered a cluster of five Class 0 objects confirming that star formation in CB34 is occurring throughout the globule. The dust continuum maps by Huard et al. (2000) clearly show that this new star generation is located in three different regions and prove the importance of further investigations aimed at studying their molecular environments. It is reasonable to expect that the three star-forming regions (SFRs) are embedded in three high-density molecular clumps hosting the star-forming processes. In the past, the molecular content of CB34 was investigated using line emissions from different species tracing the quiescent gas (e.g. Yun & Clemens 1994; Launhardt et al. 1998; Codella & Scappini 1998, and references therein) but probably due to the poor sampling and to the relatively low resolution, only two maxima in the eastern region of CB34 were detected. A step ahead was performed by Khanzadyan et al. (2002) who produced H^{13}CO$^+$ channel maps; according to the authors the maps reveal two of the three clumps, but that located in the western part of CB34 was still missed. Moreover, due to experimental difficulties, Khanzadyan et al. (2002) reported on a general morphological information on CB34 rather than an interpretation of the brightness of the features found in their spectra. In other word, the results so far obtained for CB34 call for a quantitative study of the natal molecular clumps associated with the youngest star-formation activity.

With this in mind, we carried out a multiline survey of the CB34 Class 0 cluster using millimetre wavelength emissions from molecular species tracing different physical and chemical conditions. The goal of the whole project was to investigate the relationship between the chemistry and the physical characteristics of the earliest stages of the star-forming process.

In a previous paper (Codella et al. 2002, hereafter Paper I), we presented the first results of this survey limited to the analysis of SO and SiO emissions, which are able to trace the occurrence of the outflows driven by young stellar objects (YSOs): (i) we showed that the Class 0 objects are associated with at least two SiO and SO outflows and (ii) we detected for the first time, using SO, the three molecular clumps (called A, B and C) in which the objects are embedded. Moreover, we suggested that the spatial and spectral characteristics of SiO and SO can be used to put in an evolutionary sequence the

★E-mail: codella@arcetri.astro.it

YSOs embedded in such clumps. In particular, whereas the clumps A and B are associated with high-velocity SO and SiO emissions, no wings have been detected in the clump C line profiles. The latter behaviour can be explained if the SO and SiO molecules produced at high velocities in the shocked regions are destroyed or slowed down because of the interaction with the ambient medium. Thus, the results suggested that the YSO in clump C is in a more evolved phase than the other members of the Class 0 cluster, but to confirm this indication we need to derive the SiO and SO abundances.

In the present paper we present the remaining observations in ^{12}CO (hereafter CO), ^{13}CO, C^{18}O and CS. The main aims are: (i) to analyse the gas distribution and the physical parameters of the three clumps; (ii) to study the interaction between the newly formed stars and their environment; (iii) to estimate the SO and SiO abundances and their use to derive an evolutionary sequence for the YSOs. Finally, we discuss the advantages of comparatively investigating a cluster of YSOs in the same globule compared to observing the same objects in different environments.

2 OBSERVATIONS

The observations were carried out with the Institut de Radio Astronomie Millimetrique (IRAM) 30-m telescope at Pico Veleta (Granada, Spain) during several runs in 1998 June and in 1999 January and May. Table 1 summarizes the observed molecular species, the transitions, and their rest frequencies. The main beam efficiency varies from 0.67 (at 109 GHz) to 0.39 (at 231 GHz) according to the values reported by Wild (1995). The observations were made by position switching. The pointing was checked every hour by observing nearby planets or continuum sources and it was found to be accurate to within 4 arcsec. As spectrometers, an autocorrelator (AC) split into three parts was used to allow simultaneous observations of three different transitions. Moreover, a 1-MHz filter bank, split into three parts of 2 × 256 and 512 channels, was simultaneously used. Table 1 shows the velocity resolutions provided by both back ends, AC and 1 MHz, as well as the half power beam width (HPBW), the typical system temperature ($T_{\rm sys}$), and the integration time ($t_{\rm int}$; ON+OFF source). When necessary, the AC spectra were smoothed to a lower velocity resolution (up to 0.43 km s^{-1}). The spectra were calibrated by the standard chopper wheel method and are reported here in units of main-beam brightness temperature ($T_{\rm MB}$).

3 RESULTS

3.1 The globule and the three molecular clumps

Fig. 1 shows the contour maps of the integrated $J = 1$–0 (left panel) and 2–1 (right panel) CO emissions. Fig. 2 reports the integrated emission maps of the ^{13}CO $J = 2$–1 (upper panel), C^{18}O 1–0 (middle panel) and CS 3–2 (lower panel). These maps (as well as the others presented in this paper) are centred at $\alpha_{2000} = 05^{\rm h}47^{\rm m}02\overset{\rm s}{.}1$, $\delta_{2000} = +21^{\circ}00'10''$, i.e. at the *IRAS* counterpart coordinates. The five YSOs detected by Huard et al. (2000) are indicated by filled triangles and are labelled following the authors' numbering (from 1 to 5).

The maps confirm the existence of an elongated structure. In addition, we can see that going from optically thick to thin tracers (see below for the estimate of the optical depths), three well-separated clumps associated with the brightest YSOs appear, reproducing the submillimetre dust continuum maps of Huard et al. (2000). The present results confirm what was found in the SO survey (Paper I) and consequently we call A the clump near the submillimetre sources 3 and 4, that close to source 2 is B, and the clump

Table 1. List of molecular species, transitions and observing parameters.

Molecules	Transition	Rest frequency (MHz)	HPBW (arcsec)	$T_{\rm sys}$ (K)	$t_{\rm int}$ (s)	dv (AC) (km s^{-1})	dv (1 MHz) (km s^{-1})
C^{18}O	$J = 1$–0	109782.156	22	150	240	0.11	2.73
CO	$J = 1$–0	115271.195	21	280	60	0.10	2.60
CS	$J = 3$–2	146969.047	16	285	280	0.16	2.04
^{13}CO	$J = 2$–1	220398.688	11	300	240	0.11	1.36
CO	$J = 2$–1	230537.984	10	300	60	0.10	1.30

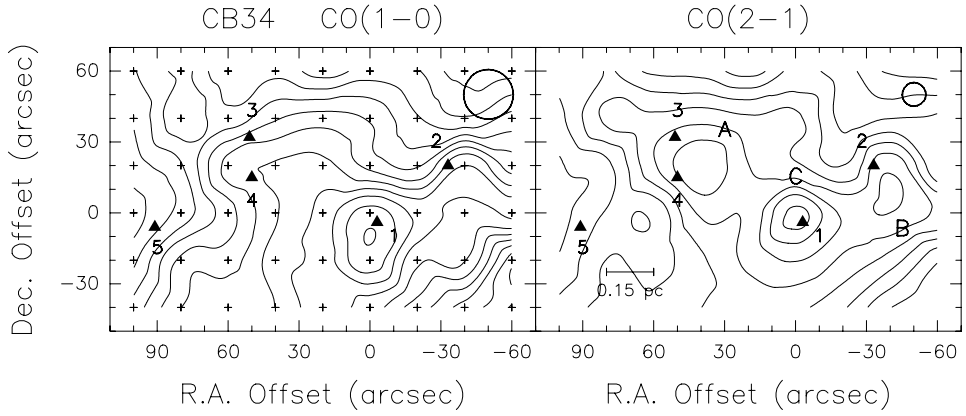

Figure 1. Contour maps of the $J = 1$–0 and $J = 2$–1 CO integrated emissions towards CB34. The empty circles show the IRAM beam (HPBW) and the small crosses mark the observed positions. The filled triangles indicate the coordinates of the submillimetre sources (Huard et al. 2000), which are numbered according to the authors. The maps are centred at the *IRAS* coordinates (see Section 3.1). The labels A, B and C indicate the three molecular clumps (see Section 3.1). The contours range from 19.0 to 49.0 K km s^{-1} (left panel), and from 19.5 to 46.5 K km s^{-1} (right panel). The first contours correspond to about 20 (left panel) and 15σ (right panel; σ is the rms of the map), whereas the steps correspond to about 3σ.

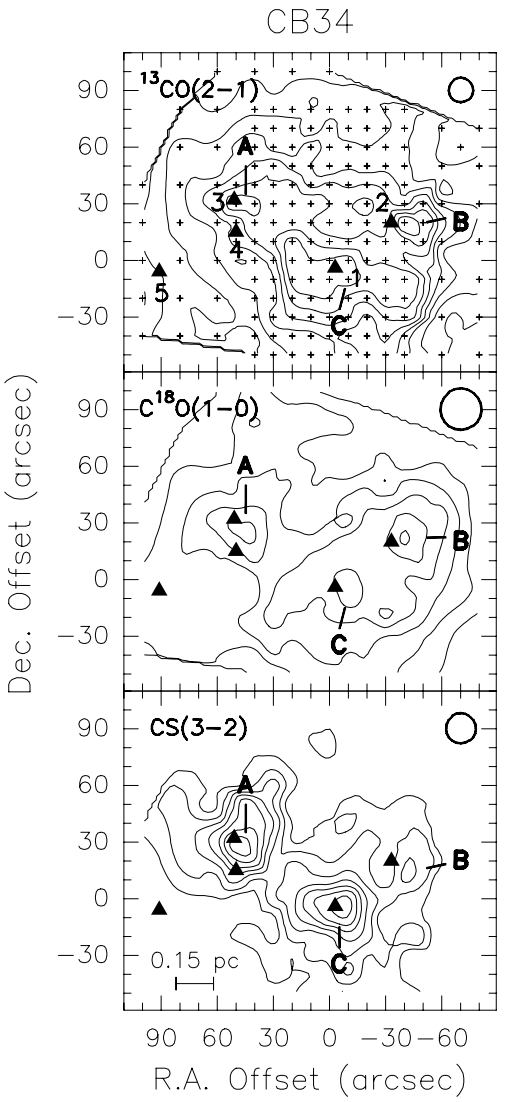

Figure 2. Contour maps of the $J = 2$–1 ^{13}CO (upper panel), $J = 1$–0 C^{18}O (middle panel), and $J = 3$–2 CS (lower panel) integrated emission towards CB34. Symbols are drawn as in Fig. 1. The contours range from 2.6 to 20.8 K km s^{-1} (upper panel), from 0.5 to 3.0 K km s^{-1} (middle panel), and from 1.0 to 7.0 K km s^{-1} (lower panel). The first contours and the steps correspond to about 4σ.

which peaks near the source 1 is called C. Previous observations of CB34 using standard tracers of high-density clumps led either to the detection of an elongated single peak structure, in CS (Launhardt et al. 1998) and in HCN (Afonso, Yun & Clemens 1998) or to a globule with two maxima corresponding to the clumps A and C, in NH_3 (Codella & Scappini 1998) and in H^{13}CO$^+$ (Khanzadyan et al. 2002). In this work we have detected for the first time the clump B using standard tracers of the molecular clumps associated with star formation. The maps show also that the submillimetre source 5 is located inside CB34, as traced by CO and its isotopes, but there is no clear indication of any association of a molecular clump with such an object. This could be due to sensitivity limitation because the source 5 is unresolved (size <15 arcsec) and is the faintest among the components of the YSO clusters; it shows a total flux of 0.18 Jy at 850 μm, whereas the other continuum objects are associated with fluxes between 0.53 and 1.40 Jy.

In order to derive the physical properties of the three clumps, we assumed as ambient emission that traced by C^{18}O. Even with the uncertainties given by the occurrence of absorption in the observed line profiles (see Fig. 3), the comparison between the CO(1–0) and C^{18}O(1–0) spectra gives an estimate of the C^{18}O optical depth, τ_{18}; values around 0.1–0.2 are obtained. On the other hand, the comparison between the CO(2–1) and ^{13}CO(2–1) emissions allows us to measure the ^{13}CO optical depth, $\tau_{13} \simeq 1$. Ratios of ^{12}C/^{13}C = 77 and ^{16}O/^{18}O = 560 (Wilson & Rood 1994) have been assumed. The derived excitation temperature is around 8 K for the three clumps. It is plausible that such a low temperature applies to the external portions of the clumps rather than to the regions near the new stars. A total CO column density of $\simeq 1 \times 10^{18}$ cm^{-2} is also derived for the three ambient components from the C^{18}O peaks assuming local thermodynamic equilibrium (LTE) conditions. For the total column densities of CS, the following LTE values are calculated: 4.1×10^{13} (A), 1.6×10^{13} (B), and 2.6×10^{13} cm^{-2} (C).

The sizes and masses of the three clumps are calculated by using the C^{18}O and CS emissions. The beam deconvolved FWHM sizes are $\simeq$30 arcsec (0.22 pc at a distance of 1500 pc; Launhardt & Henning 1997) for A and B, and 36 arcsec (0.26 pc) for C. The masses are derived assuming homogeneous spheres and the hydrogen densities calculated from the large velocity gradient (LVG) analysis of the SO ambient emission (Paper I): 2×10^5 (A and C) and 5×10^4 cm^{-3} (B). The following values are computed: 52 (A), 13 (B) and 94 $M_\odot$ (C). These estimates, as expected given the assumptions, are close to those obtained from SO; the small discrepancies (less than a factor of 3) are due to the differences between the sizes measured from the SO, C^{18}O and CS data. The comparison of the masses derived here for the three clumps with those calculated from dust emission by Huard et al. (2000) shows that for clumps A and B the present estimates are larger by a factor of 2–4. The difference is higher for clump C, where the mass derived from molecular emission is ∼20 times larger than that derived from dust emission. These differences can be attributed to the large uncertainties associated with such measurements and to the different procedures used, as discussed in Section 3.2 of Paper I. For completeness, the virial masses have also been calculated using the standard procedure (e.g. MacLaren, Richardson & Wolfendale 1988): 60 (A), 41 (B) and 71 $M_\odot$ (C). Finally, it is worth noting that the sum of the masses of the three clumps, 159 $M_\odot$, is in good agreement with the previous estimate of 170 $M_\odot$ given by Launhardt et al. (1998) for the CB34 cloud and based on CS.

3.2 Line profiles

The complexity of the observed region is confirmed by the variety of the line profiles of Fig. 3, where typical lines observed towards the three clumps A, B and C are reported. The C^{18}O profiles are the only ones which do not show high-velocity emission features and thus can be used to obtain the ambient local standard of rest (LSR) velocities through a Gaussian fit. The dashed vertical lines correspond to the observed values, which are reported in Table 2 together with the derived spectra parameters: peak $T_{\rm MB}$, noise of the spectrum (rms), FWHM linewidth and integrated flux (F). On the other hand, the CO, ^{13}CO, C^{18}O and CS lines show prominent emission wings emission confirming the occurrence of outflows (see Section 3.3).

Focusing the attention on the ambient velocities, e.g. where C^{18}O emits, it is possible to see that while the optically thin lines of C^{18}O and CS have an almost Gaussian shape, the profiles of the

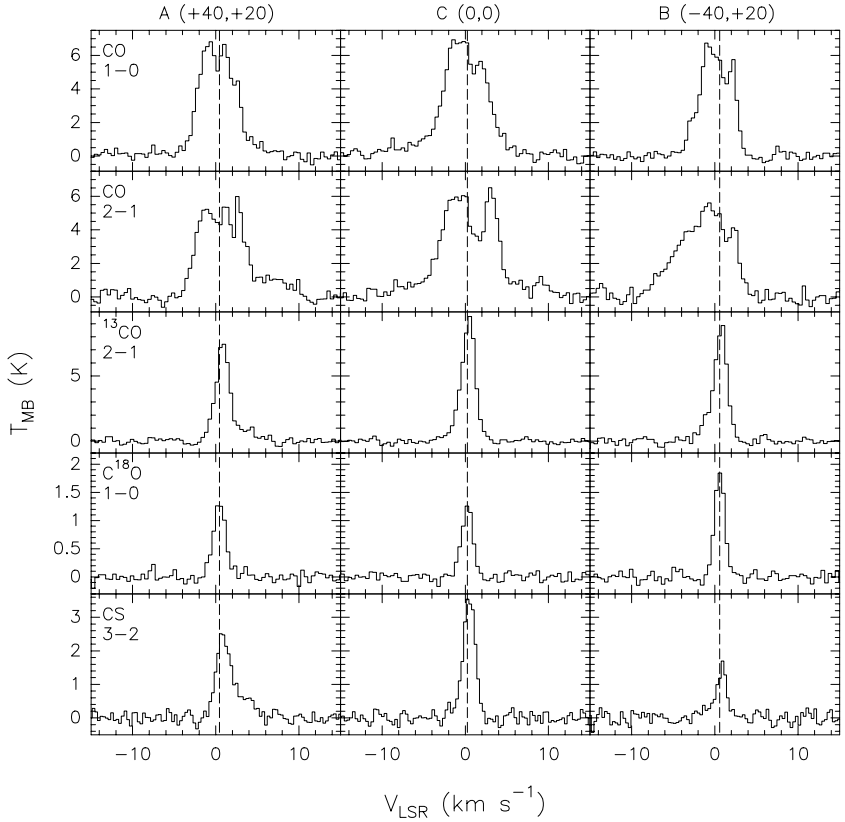

Figure 3. Examples of CO, ^{13}CO, C^{18}O and CS line profiles observed towards the three clumps located in the CB34 globule (see Section 3.1). Molecular species, transition and angular offset are indicated. The dashed lines denote the ambient LSR velocity, according to the C^{18}O measurements.

Table 2. Observed spectra parameters towards selected CB34 map positions (see text).

Transition	Offset (arcsec)	T_{MB} (K)	rms (K)	v_{LSR} (km s^{-1})	FWHM[a] (km s^{-1})	F (K km s^{-1})
CO(1–0)	0,0	6.79(0.49)	0.26	−0.11 (0.04)	5.80 (0.41)	45.54 (1.05)
	−40,+20	6.49 (0.71)	0.18	+0.07 (0.03)	4.49 (0.41)	27.58 (0.73)
	+40,+20	6.71 (0.60)	0.24	+0.16 (0.08)	4.97 (0.41)	36.14 (0.97)
CO (2–1)	0,0	6.01 (0.93)	0.36	+0.33 (0.07)	7.72 (0.41)	49.58 (1.46)
	−40,+20	5.17 (0.51)	0.35	−1.10 (0.08)	7.14 (0.41)	39.01 (1.42)
	+40,+20	5.37 (0.75)	0.29	+0.72 (0.07)	6.40 (0.41)	38.25 (1.17)
^{13}CO (2–1)	0,0	9.22 (0.46)	0.16	+0.39 (0.02)	2.00 (0.03)	20.78 (0.50)
	−40,+20	8.44 (0.60)	0.23	+0.68 (0.02)	1.95 (0.05)	18.20 (0.72)
	+40,+20	6.84 (0.28)	0.18	+0.82 (0.02)	1.82 (0.04)	17.52 (0.57)
C^{18}O (1–0)	0,0	1.26 (0.05)	0.06	+0.24 (0.03)	1.57 (0.07)	2.20 (0.08)
	−40,+20	1.89 (0.09)	0.07	+0.59 (0.02)	1.41 (0.05)	2.86 (0.10)
	+40,+20	1.31 (0.07)	0.07	+0.45 (0.03)	1.72 (0.08)	2.34 (0.10)
CS (3–2)	0,0	3.63 (0.13)	0.14	+0.49 (0.02)	1.71 (0.05)	6.79 (0.25)
	−40,+20	1.47 (0.15)	0.16	+0.81 (0.05)	1.50 (0.15)	2.87 (0.29)
	+40,+20	2.34 (0.21)	0.11	+1.06 (0.05)	2.51 (0.21)	6.98 (0.20)

[a]The FWHM values have been obtained by fitting a Gaussian to the lines with the exception of the CO transitions whose profiles are affected by wings and absorptions; in these cases, we have read off the linewidth using the cursor.

CO thicker transitions present dips which suggest the existence of velocity gradients in CB34. In addition, the ^{13}CO(2–1) lines are stronger than the corresponding CO lines. These findings could be due to the absorption from an external cooler layer enveloping the three clumps. This explanation is supported by the fact that the dips are still present away from the clump centre positions, consistently with the absorption being due to a structure more extended than the clumps and coinciding with the central part of CB34.

Furthermore, the dips of the profiles, reported in Fig. 3, especially those of the clumps C and B are redshifted with respect to the systemic velocity, suggesting that the absorbing material follows a velocity trend. A possible explanation is to be found in Fig. 4. In the upper and lower panels, we report typical spectra representative of the SW and NE regions, respectively, which have been obtained by summing the profiles belonging to about 30 × 30 arcsec^2 regions of CB34. It can be seen that, whereas a redshifted dip is present towards

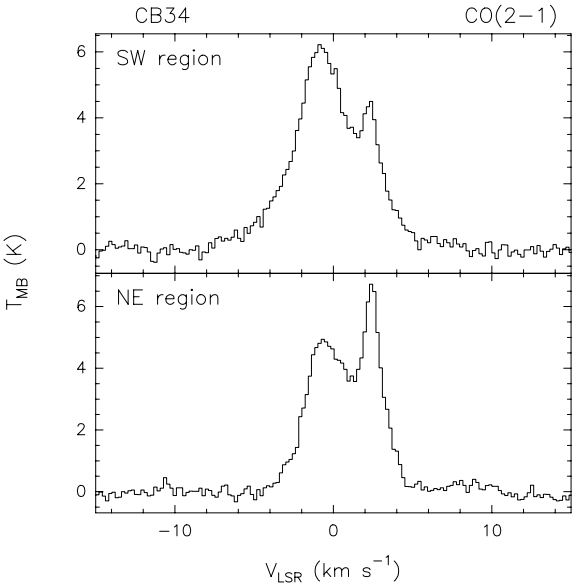

Figure 4. Carbon monoxide $J = 2$–1 spectra of the CB34. The upper panel shows the profile obtained by summing the spectra observed towards the SW region, while the spectrum reported in the lower panel refers to the NE region (see text).

SW, a blueshifted absorption appears in the NE region. This result suggests that either CB34 is rotating or that different parts of it are associated with different velocities.

3.3 The multiple outflows

The spectra reported in Fig. 3 clearly confirm the occurrence of molecular outflows in the high-velocity CO emission which is detected between about -7 and $+10$ km s^{-1}. In order to study the kinematics of the outflow motions, the channel map of the $J =$ 2–1 CO emission is reported in Fig. 5. The ambient LSR velocity emission, as defined by $C^{18}O$, is centred around the -1 and $+1$ km s^{-1} panels. The data presented in Fig. 5 are fully in agreement with the CO picture given by Khanzadyan et al. (2002) and show that the high-velocity structure of CB34 is quite complex. Moreover, the present CO maps show several clumps at different velocities. In particular, two blueshifted clumps (hereafter called Blue1 and Blue2; see the -7 km s^{-1} panel) and at least three redshifted clumps (Red1, Red2 and Red3; see the $+5$ km s^{-1} panel) have been detected. These clumps are spatially associated with the YSOs 1, 2, 3 and 4; again, YSO 5 distinguishes itself from the the other components of the CB34 cluster because it shows no clear association with high-velocity gas. The present data do not allow us to say whether this is due to lack of sensitivity, confusion, the different nature or evolutionary stage of the object.

In trying to understand which YSOs are driving the observed outflows, we note in Fig. 5 an intense outflow activity associated with YSOs 1 and 2. In particular, we observe a blueshifted elongated NW–SE structure containing the Blue1 and Blue2 clumps aligned along the direction of the two YSOs, which is, in practice, the same line traced by the H_2 jet called H by Khanzadyan et al. (2002). Looking for a redshifted counterpart, we find a less defined structure mainly located SE of YSO 1 and associated with the Red2 clump. Moreover, the indication of another red clump not fully sampled by the present maps can be found at the (-60 arcsec, 0 arcsec) offset. In the north-eastern portion of CB34, a well-elongated redshifted structure starting from the coordinates of YSOs 3 and 4 towards NW has been detected. This emission is associated with the Red1 and Red3 clumps and is roughly aligned along the direction of the N H_2 jet (Khanzadyan et al. 2002). The blueshifted emission shows no clear counterparts but reports an extended and quite bright emission which is visible in the -3 km s^{-1} panel.

In summary, the channel maps indicate a high degree of confusion and it is risky to combine the outflows and the YSOs on a one-to-one basis and to derive geometries. However, the present CO maps confirm that a multiple outflow activity is present in CB34, which is associated with the three clumps A, B and C hosting the Class 0 cluster and is driven in particular by YSOs 1, 2, 3 and 4.

4 DISCUSSION

4.1 Outflow energetics

In order to derive a rough estimate of the energetics of the outflows driven by the Class 0 sources, given the complexity of CB34, we arbitrarily sample three regions of about 40 × 40 arcsec^2 centred at the positions of the three SFRs, A, B and C. By comparing the line profiles, e.g. reported in Fig. 3, we define as red and blue wings the region of velocities where no $C^{18}O$ emission has been detected.

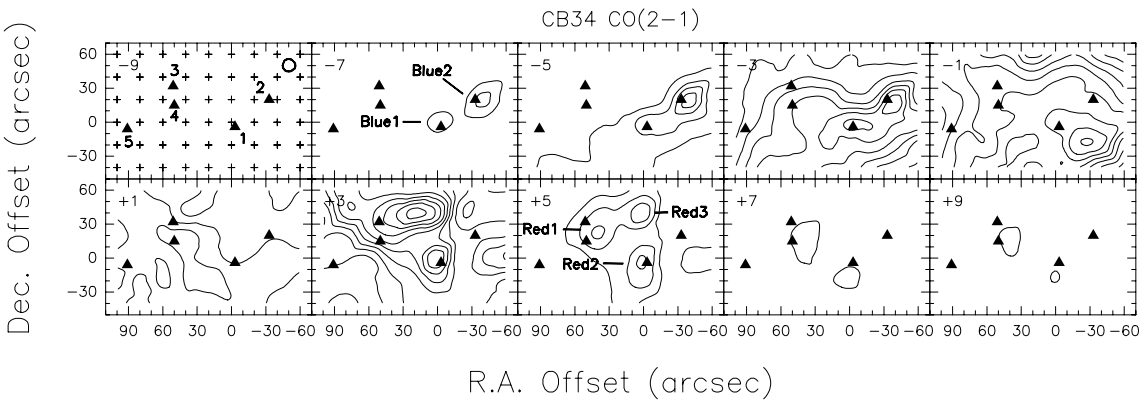

Figure 5. Channel map of the CO $J = 2$–1 emission towards CB34. Each panel shows the emission integrated over a velocity interval of 2 km s^{-1} centred at the value given in the left corner. Symbols are drawn as in Fig. 1, while the labels indicate different blue (Blue1 and Blue2) and red (Red1, Red2 and Red3) components of the molecular outflow (see Section 3.2). The contours range from 1.25 to 12.50 K km s^{-1}. The first contours and the steps correspond to about 5σ.

As done for the ambient component, by comparing the CO(2–1) and ^{13}CO(2–1) spectra, the optical depth τ_{13} is derived. The ^{13}CO emission is optically thin in all the three sampled regions with values around 0.05–0.20. The wing excitation temperature for the three clumps is estimated to be in the 8–11 K range, thus showing slightly higher values than those derived for the ambient line components.

Using standard methods (Lada 1985) and the derived optical depths and excitation temperatures, the dynamical parameters of the CB34 outflows are estimated. The total masses (red and blue) are about 8 (A), 4 (B) and 7 $M_\odot$ (C), while the outflow CO column densities are 3.8×10^{18} (A and B) and 1.6×10^{18} cm^{-2} (C). The momentum results $P \simeq 27$ (A), 13 (B) and 23 $M_\odot$ km s^{-1} (C) and the kinetic energy $E_{\rm kin} \simeq 2 \times 10^{45}$ (A), 4×10^{44} (B) and 1×10^{45} erg (C). A dynamical time-scale of the outflows in the range 10^4–10^5 yr is deduced. This allows us to estimate the force required to drive the outflows, $F \simeq 2$–4×10^{-4} $M_\odot$ km s^{-1} yr^{-1}, the mechanical luminosity $L_{\rm mech} \simeq 0.10$ (A and B) and 0.14 $L_\odot$(C), and the mass-loss rates $\dot{M} \simeq 5 \times 10^{-5}$ (A and B), 1×10^{-4} $M_\odot$ yr^{-1} (C), calculated by dividing the outflow mass by its age. Because no clear geometry can be derived for the outflow motions, no correction due to the inclination to the plane of the sky has been assumed.

In order to compare these values with those given by Yun & Clemens (1994), who calculated the dynamical parameters assuming a single outflow, a distance of 600 pc, a flow velocity of 100 km s^{-1}, and an optical depth of 3, we sum the contributions from the outflows detected towards the three clumps of CB34. We obtain a total luminosity $L_{\rm mech} \sim 0.3$ $L_\odot$ and a total momentum flow rate $F \sim 8 \times 10^{-4}$ $M_\odot$ km s^{-1} yr^{-1}. These estimates are larger by an order of magnitude than those by Yun & Clemens (1994), once scaled to a distance of 1500 pc and to the CO velocities they observed; see the estimates given by Khanzadyan et al. (2002). Such a discrepancy is due to the fact that the CO spectra reported here show emission in the -7 to $+10$ km s^{-1} range, i.e. at velocities higher than the values ± 5 km s^{-1} used by Khanzadyan et al. (2002), and that the present CO spectra give optical depths larger than 3.

A comparison between the masses and the energetics of the outflows located around the three SFRs in CB34 does not show any definite difference and thus they cannot be used to put the corresponding Class 0 YSOs in an evolutionary sequence. In other words, we are observing three outflow regions with $F = 3 \times 10^{-4}$ $M_\odot$ km s^{-1} yr^{-1}, $L_{\rm mech} \simeq 0.1$ $L_\odot$, and $\dot{M} \simeq 8 \times 10^{-5}$ $M_\odot$ yr^{-1}. The comparison of these values with those taken from the literature (e.g., Cabrit & Bertout 1992; Shepherd & Churchwell 1996; Smith 2000, and references therein) place these outflows close to others driven by $\sim$10 $L_\odot$ sources. In order to estimate the uncertainties due to the lack of a geometry correction, we assume a quite close inclination to the plane of the sky, 20°, and obtain $F = 3 \times 10^{-3}$ $M_\odot$ km s^{-1} yr^{-1}, $L_{\rm mech} \simeq 2$ $L_\odot$, and $\dot{M} \simeq 2 \times 10^{-4}$ $M_\odot$ yr^{-1}. In this case, the outflows should be driven by sources with higher luminosities, close to 100 $L_\odot$. These values are in good agreement with the luminosities of the YSOs derived by Huard et al. (2000) from their submillimetre dust emission, 10–100 $L_\odot$.

Finally, it is worth noting that Shepherd & Churchwell (1996) derived a relationship between the masses and the dynamical time-scales of molecular outflows driven by YSOs of all luminosities. Thus, a parameter which does not depend on the inclination of the flow to the plane of the sky such as the mass can be used to estimate the outflow age. By using the masses derived for the A, B and C SFRs and by assuming that the YSOs have luminosities less than 100 $L_\odot$, we obtain time-scales between 5×10^4 and 10^5 yr, in agreement with the kinematical estimate from the distribution of the outflowing material with respect to the position of the YSOs (see above).

4.2 SiO and SO abundances

As reported in Section 1, the results of Paper I have suggested that the spatial and spectral properties of the SO and SiO emissions in CB34 can be used to put the YSOs in an evolutionary sequence. In fact, those results have indicated the possibility to date the YSOs through the chemical characteristics of the neighbouring gas affected by the occurrence of molecular outflows. Using the line profiles and the line intensities of SO and SiO, two distinct regimes have been identified for SO and SiO: a low-velocity emission associated with the ambient velocity, and a high-velocity emission associated with the outflows and detected only towards clumps A and B. The lack of a high-velocity regime in clump C has been interpreted as an indication of a more evolved evolutionary phase for the YSO contained in such a clump. With the help of the present data, we can now estimate the SO and SiO fractional abundances for each regime by comparing the column densities of such molecules (Paper I) with those of CO, ^{13}CO and C^{18}O and by assuming $[{\rm CO}/{\rm H_2}] = 10^{-4}$.

For the low-velocity component, the C^{18}O isotopomer is used and the following SO abundances are found: 5×10^{-9} (A and C) and 2×10^{-9} (B). Only clump C is associated with a SiO low-velocity component; the SiO abundance is derived to be about 1×10^{-10}. For the high-velocity component, the comparison with CO and ^{13}CO yields SO abundances, 2×10^{-7} (A) and 9×10^{-7} (B), and SiO abundances, 5×10^{-9} (A) and 2×10^{-8} (B). No high-velocity component had been detected towards clump C. Thus, we find an increase of the abundances of SiO at velocities associated with the outflows (high-velocity regime) with respect to the values calculated for the SiO component with velocities similar to the ambient one. In fact, the SiO abundance in clumps A and B are higher by 50 and 200, respectively, than for clump C. Similarly, by comparing the SO abundance for the two regimes in the same clump we find an increase at high velocities of a factor of 40 (A) and 450 (B) with respect to the value regarding the narrow SO component at ambient velocities.

The fact that we are comparing YSOs of a cluster in the same globule suggests the use of the different abundances calculated here to give a rough estimate of the time-scale $t_{\rm des}$ in which the molecules produced or injected in the gas phase at high velocities by a shocked chemistry are destroyed. In particular, the attention is focused on SiO, which presents the advantage of tracing only the shocked gas, whereas the SO spectra can be confused by emission from the ambient medium. The YSO in clump C is thought to be in a more evolved stage and is associated with the lowest SiO abundance. If we take into account that (i) the YSOs of the CB34 cluster have been classified as Class 0 objects, whose typical age is $\sim 10^4$–10^5 yr (e.g. André & Montmerle 1994; Ward-Thompson et al. 1994, and the recent work of Visser, Richer & Chandler 2002), (ii) the derived outflow ages for CB34 are 10^4–10^5 yr (without geometry correction), and (iii) the outflows are commonly thought to consist of ejections with wide intervals between them (e.g. Schilke et al. 1997), then it is tempting to derive $t_{\rm des} < 10^4$–10^5 yr for SiO. It is interesting to note that this estimate is in good agreement with the value given, for example, by Bergin, Neufeld & Melnick (1998) for the time-scale associated with the removal of SiO from the gas phase by direct accretion on to grains in a $\sim 10^5$ cm^{-3} density medium (van Dishoeck & Blake 1998). Moreover, Pineau des Forêts, Flower & Chièze (1997) have shown that the SiO molecules present in the gas phase can be efficiently destroyed by reacting with OH, leading to a

production of SiO_2 in the same time-scale (see also Schilke et al. 1997). Naturally, this estimate can be made only if we assume that the physical conditions associated with the three clumps and the energetics of the CB34 outflows are the same. Unfortunately, the present data do not allow us to assess if these conditions are fully satisfied. However, the present results seem to indicate that the three clumps A, B and C (see Section 3.1) as well as the outflows (see Section 4.1) have similar characteristics.

5 SUMMARY

We have studied the molecular cloud associated with the young cluster of Class 0 YSOs located in the globule CB34 through a multiline survey at millimetre wavelengths. The main findings are as follows.

(i) The CO, ^{13}CO, C^{18}O and CS maps confirm the existence of an elongated structure containing three well-separated clumps (called A, B and C) with sizes of about 0.25 pc, temperatures of about 8 K, and associated with the brightest YSOs, reproducing well the submillimetre dust continuum distribution (Huard et al. 2000). Clump B has been detected here for the first time using standard tracers of molecular clumps.

(ii) While the optical thin lines of ^{13}CO, C^{18}O and CS have Gaussian shapes, the profiles of the CO thicker transitions present dips, which suggest an absorption due to an external cooler layer enveloping the three clumps. Moreover, the dips are blueshifted or redshifted with respect to the ambient velocity depending on the map position, indicating either that CB34 is rotating or that it is associated with different velocities.

(iii) The CO data show that the high-velocity structure of CB34 is quite complex. The degree of confusion is high with several clumps at different velocities. The outflow activity is concentrated around the brightest YSOs and associated with the three molecular clumps. Redshifted and blueshifted elongated structures as well as less defined lobes are observed, indicating the occurrence of multiple outflows.

(iv) A comparison between the masses and the energetics of the outflow motions located around the three SFRs (A, B and C) in CB34 does not show any definite difference. In fact, we observe regions with $\simeq 3 \times 10^{-4}$ M$_\odot$ km s^{-1} yr^{-1}, $L_{\rm mech} \simeq 0.1$ L$_\odot$, and $\dot{M} \simeq 8 \times 10^{-5}$ M$_\odot$ yr^{-1}, which suggest a typical luminosity of 10 L$_\odot$ for the driving Class 0 YSOs.

(v) The fractional abundances of SiO and SO, whose detection has been reported in Paper I, have been calculated. For these molecules two distinct regimes are present: a low-velocity emission at ambient velocities with X(SiO) $\simeq 1 \times 10^{-10}$ and X(SO) $\simeq$2–5 $\times 10^{-9}$, and a high-velocity emission associated with the outflows where the fractional abundances increase up to $\simeq 2 \times 10^{-8}$ and 9×10^{-7}, respectively. The YSO in clump C does not present the high-velocity regime, and thus is thought to be in a more evolved stage, where the molecules produced at high velocities in the shocked regions are destroyed or slowed down due to the interaction with the ambient gas.

In conclusion, we show that in the CB34 SFRs the different Class 0 objects cannot be distinguished upon the physical characteristics of their natal molecular clumps or of the associated molecular outflows. On the other hand, the abundances as well as the spectral characteristics of molecules whose chemistry is strongly affected by the occurrence of molecular outflows, such as SO and SiO, can be used to further specify the characteristics of the objects defined as Class 0, from their dust continuum emission properties. It is worth noting that this picture is in agreement with the classification scheme of the outflow evolution given by Bachiller & Tafalla (1999) who have proposed that outflows driven by Class 0 objects can be distinguished from their chemical properties. In particular, a chemical-rich phase should be associated with Class 0 YSOs which alter the chemistry of the surrounding medium through the mass-loss process. The present results, based on a single cluster, call for further high-angular-resolution observations in order to be confirmed on a statistical basis.

ACKNOWLEDGMENTS

We wish to thank R. Bachiller, M. Benedettini and R. Cesaroni for helpful discussions and suggestions. We also thank the referee for the contribution to the improvement of the paper.

REFERENCES

Afonso J. M., Yun J. L., Clemens D. P., 1998, AJ, 115, 1111
André P., Montmerle T., 1994, ApJ, 420, 837
Alves J. F., Yun J. L., 1995, ApJ, 438, L107
Bachiller R., Tafalla M., 1999, in Lada C. J., ed., The Physics of Star Formation and Early Stellar Evolution, NATO Advanced Science Institute. Kluwer, Dordrecht
Bergin E. A., Neufeld D. A., Melnick G. J., 1998, ApJ, 499, 777
Bok B. J., Reilly E. F., 1947, ApJ, 105, 255
Cabrit S., Bertout C., 1992, A&A, 261, 274
Clemens D. P., Barvainis R. E., 1988, ApJS, 68, 257
Clemens D. P., Yun J. L., Heyer M. H., 1991, ApJS, 75, 877
Codella C., Scappini F., 1998, MNRAS, 298, 1092
Codella C., Scappini F., Bachiller R., Benedettini M., 2002, MNRAS, 331, 893 (Paper I)
Huard T. L., Weintraub D. A., Sandell G., 2000, A&A, 362, 635
Khanzadyan T., Smith M. D., Gredel R., Stanke T., Davis C. J., 2002, A&A, 383, 502
Lada C. J., 1985, ARA&A, 23, 267
Launhardt R., Henning Th., 1997, A&A, 326, 329
Launhardt R., Evans II N. J., Wang Y., Clemens D. P., Henning Th., Yun J. L., 1998, ApJS, 119, 59
MacLaren I., Richardson K. M., Wolfendale A. M., 1988, ApJ, 333, 821
Moreira M. C., Yun J. L., 1995, ApJ, 454, 850
Pineau des Forêts G., Flower D. R., Chièze J.-P., 1997, in Reipurth B., Bertout C., eds, Proc. IAU Symp. 182, Herbig–Haro Flows and the Birth of Low Mass Stars. Kluwer, Dordrecht, p. 199
Schilke P., Walmsley C. M., Pineau des Forêts G., Flower D. R., 1997, A&A, 321, 293
Shepherd D. S., Churchwell E., 1996, ApJ, 472, 225
Smith M. D., 2000, Irish, AJ, 25, 27
van Dishoeck E. F., Blake G. A., 1998, ARA&A, 36, 317
Visser A. E., Richer J. S., Chandler C. J., 2002, AJ, 124, 2756
Ward-Thompson D., Scott P. F., Hills R. E., André P., 1994, MNRAS, 268, 276
Wild W., 1995, The 30-m manual – A handbook for the IRAM 30-m Telescope, IRAM report
Wilson T. L., Rood R., 1994, ARA&A, 32, 191
Yun J. L., Clemens D. P., 1994, ApJS, 92, 145

This paper has been typeset from a TEX/LATEX file prepared by the author.